



HIERARCHIC MODELING OF HEAT EXCHANGER THERMAL HYDRAULICS

Andrej Horvat, Boštjan Končar
"Jožef Stefan" Institute
Reactor Engineering Division
Jamova 39, SI-1111 Ljubljana, Slovenia
andrej.horvat@ijs.si, bostjan.koncar@ijs.si

ABSTRACT

Volume Averaging Technique (VAT) is employed in order to model the heat exchanger cross-flow as a porous media flow. As the averaging of the transport equations lead to a "closure" problem, separate relations are introduced to model interphase momentum and heat transfer between fluid flow and the solid structure. The hierarchic modeling is used to calculate the local drag coefficient C_d as a function of Reynolds number Re_h . For that purpose a separate model of REV is built and DNS of flow through REV is performed. The local values of heat transfer coefficient h are obtained from available literature. The geometry of the simulation domain and boundary conditions follow the geometry of the experimental test section used at U.C.L.A. The calculated temperature fields reveal that the geometry with denser pin-fins arrangement (HX1) heats fluid flow faster. The temperature field in the HX2 exhibits the formation of thermal boundary layer between pin-fins, which has a significant role in overall thermal performance of the heat exchanger. Although presented discrepancies of the whole-section drag coefficient \bar{C}_d are large, we believe that hierarchic modeling is an appropriate strategy for calculation of complex transport phenomena in heat exchanger geometries.

1 INTRODUCTION

Despite the crucial role of heat exchangers in industrial and especially in nuclear installations, there is still a lot of empiricism involved in their design. Although the present guidelines provide an ad-hoc solution to the design problems, a unified approach based on simultaneous modeling of thermal hydraulics and solid structure behavior has not been proposed yet. As a consequence, designs are overly constrained with a resulting economic penalty. Therefore, a number of research groups (e.g. M.I.T, U.C.L.A in U.S.A., C.E.A. in France, J.S.I. in Slovenia etc.) are currently trying to develop a unifying scientific procedure for optimization of heat exchanger geometry, applying the most advanced computational techniques.

In the present paper, the integral thermo-hydraulic equations, developed by Travkin and Catton [1], are solved using a hierarchic modeling of fluid and heat flow behavior. In order to calculate the steady-state heat transfer in a heat exchanger a numerical code based on Volume Averaging Technique (VAT) is constructed. Due to volumetric averaging, the code describes the cross-flow inside a heat exchanger as porous media flow. Such description enables the code to be fast running, but still capable of resolving details of temperature and heat flow

distribution. Nevertheless, the interaction between fluid flow and the heat transferring solid structure has to be described with additional relations, which introduce two empirical coefficients (drag coefficient C_d and heat transfer coefficient h).

In order to obtain the local distribution of drag coefficient C_d , the separate model of Representative Elementary Volume (REV) of the heat exchanger is made. The CFX-5 computer code is used to perform the Direct Numerical Simulations (DNS) of the fluid flow inside REV. The calculated three-dimensional distributions of velocity are then used to determine the local drag coefficient C_d as a function of Reynolds number Re_h . For the same purpose, the experimental data are used to determine the local heat transfer coefficient h as a function Re_h . These functions are then used as an input data for the integral thermo-hydraulic model.

To test the capability of VAT algorithm, the simulations were performed for two-different geometries, which closely follow the geometry configurations, experimentally studied in the Morrin-Martinelli-Gier Memorial Heat Transfer Laboratory at U.C.L.A. .

2 MODELING APPROACH

The airflow across an isothermal solid structure can be described with basic transport equations of mass, momentum and heat. In order to develop a unified approach for heat exchanger calculations, the transport equations are averaged over a REV using VAT (see Horvat [4] for details). As the details of interphase exchange are lost due to the averaging procedure, additional relations are needed to capture the exchange of momentum and heat between fluid flow and the solid structure. The averaging procedure results in separate temperature variables for each phase or component, therefore, the described model is called a Separate-Phase Porous Media Flow Model (SPPMFM).

To further simplify the simulated system, flow is taken as unidirectional with a constant pressure drop. As a consequence, the velocity changes only in the spanwise directions (y and z). This means that the streamwise pressure gradient across the entire simulation domain is balanced with hydrodynamic resistance of the structure and with shear stress. Thus the momentum equation can be written in differential form as:

$$-\alpha_f \mu_f (\partial_y \partial_y u_f + \partial_z \partial_z u_f) + \frac{1}{2} C_d \rho_f u_f^2 S = \frac{\Delta p}{L} \quad , \quad (1)$$

where u_f is the velocity of fluid phase and α_f is a fluid phase fraction. The momentum transfer between fluid flow and the solid structure is modeled with a quadratic velocity relation, where the parameter C_d depends on local Reynolds number.

The temperature field of the fluid phase is formed as a balance between thermal convection in the streamwise direction, thermal diffusion and heat transfer from solid to the fluid phase. Thus, a differential form of energy equation for the fluid phase is:

$$\alpha_f \rho_f c_f u_f \partial_x T_f = \alpha_f \lambda_f (\partial_x \partial_x T_f + \partial_y \partial_y T_f + \partial_z \partial_z T_f) - h(T_f - T_s) S \quad , \quad (2)$$

where T_f and T_s are temperatures of fluid and solid phase, respectively. The heat transfer between the solid and the fluid phase is modeled as a linear relation between both phase temperatures, where h is a local heat transfer coefficient.

The Eqs. (1) and (2) are written with phase averaged variables to describe the steady-state transport of momentum and heat in porous media flow. To close the system of equations, separate correlations for local values of the drag coefficient C_d and the heat transfer

coefficient h are required. These coefficients can be determined from the Direct Numerical Simulation (DNS) or from the Large-Eddy Simulation (LES) of the flow through REV. Likewise, the available experimental data can be used to obtain the required drag and heat transfer coefficients.

3 HIERARCHIC MODELING

In the presented study the DNS of the fluid flow through the Representative Elementary Volume (REV) were performed with the CFX-5 code (Fig. 1a) in order to determine the local values of drag coefficient C_d .

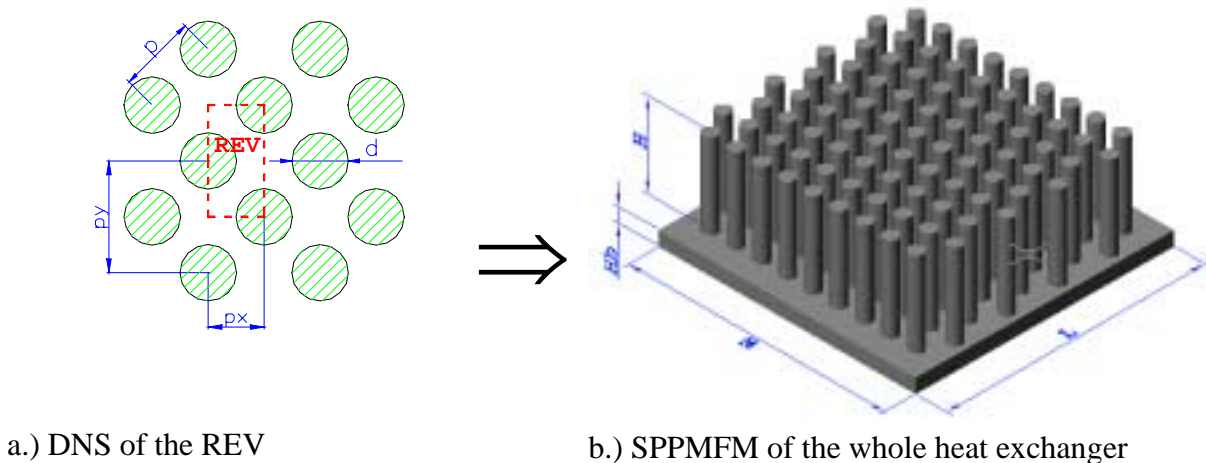


Figure 1: Principle of hierarchic modeling.

Two-different geometries of REV, with the same pin-fin diameter $d = 0.003175\text{m}$ (0.125"), were considered in our study. The first geometry (HX1) has a pitch-to-diameter ratio $p_x/d = 1.06$ in the streamwise direction and $p_y/d = 2.12$ in the transverse direction. The pitch-to-diameter ratios for the second geometry (HX2) are $p_x/d = 1.636$ and $p_y/d = 3.272$ in the streamwise and in the transverse direction, respectively. The height of the REV was 0.005 m in both cases.

Examples of pressure and velocity fields of the fluid flow through REV, calculated with DNS, are presented in Fig. 2.

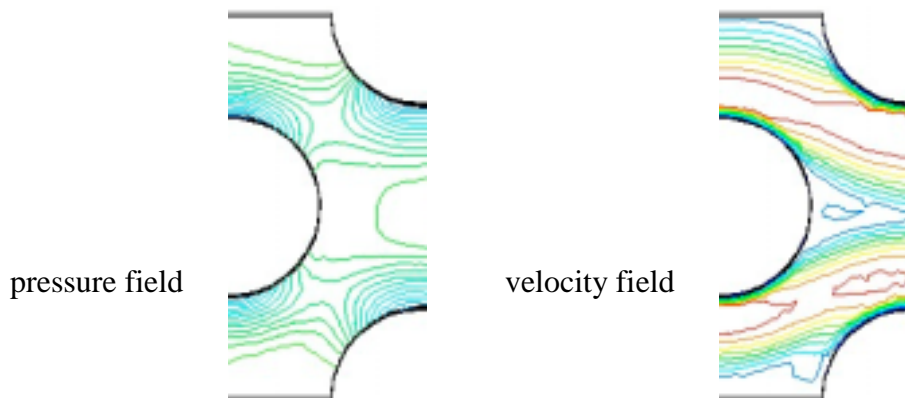


Figure 2: DNS calculation in REV, HX1, $u_c = 5.55$.

DNS was performed for 8 different inflow velocities u_c for each considered geometry. The calculated cases are summarized in Table 1.

Table 1: Summary of inflow velocities for DNS of flow through the REV.

	Inflow velocity u_c [m/s]							
HX 1	0.577	0.908	1.33	1.95	2.76	4.41	5.55	6.64
HX 2	0.559	0.881	1.29	1.90	4.15	6.13	7.64	8.53

Based on the calculated three-dimensional velocity distributions in the REV, the local values of drag coefficient C_d are obtained as:

$$C_d = \frac{2\Delta p^*}{\rho_f (u_f)^2} \left(\frac{A_c}{A_o} \right), \quad (3)$$

where A_c is the inflow and A_o the interface area. From the local distribution of fluid velocity u_f and drag coefficient C_d , a correlation between the local values of drag coefficient C_d (Eq. 3) and Reynolds number Re_h is developed. This correlation is then used to close the momentum equation (Eq. 1) of SPPMFM.

The local heat transfer coefficient h , which is required to close the energy equation (2), can be obtained using a similar procedure. As we encounter difficulties at implementing the thermal periodic boundary conditions, the correlation between local values of heat transfer coefficient h and Reynolds number Re_h is rather taken from the available literature (Žukauskas and Ulinskas [2] and Kay and London [3]).

4 SIMULATION DOMAIN

Both geometries (HX1 and HX2) were studied with the same boundary conditions. They follow the geometry of the experimental test sections used in the Morrin-Martinelli-Gier Memorial Heat Transfer Laboratory at University of California, Los Angeles, where conjugate heat transfer from electronic device heat sink was investigated (Rizzi et al. [5]).

4.1 Geometry

The common geometrical arrangement of both simulation domains is seen in Fig. 1b. The HX1 consists of 31 rows of pin-fins in the streamwise and transverse directions. The length L and width W of HX1 simulation domain are 0.1044m. The HX2 arrangement is less dense and consists of 21 pin-fins in the streamwise and transverse directions with domain length L and width W of 0.1091m. The height H is 0.0381m in both cases.

4.2 Boundary conditions

The no-slip boundary conditions for the momentum Eq. (1) are implemented for all 4 walls parallel with the flow direction:

$$u_f(0, z) = 0, \quad u_f(W, z) = 0, \quad u_f(y, 0) = 0, \quad u_f(y, H) = 0 \quad (4)$$

As a flow driving force, the whole-section pressure drop Δp is prescribed.

For the fluid-phase energy equation (2), inflow and the bottom wall of the simulation domain were taken as isothermal:

$$T_f(0, y, z) = T_{in}, \quad T_f(x, y, 0) = T_g, \quad (5)$$

whereas the other walls were considered as adiabatic:

$$\partial_x T_f(L, y, z) = 0, \quad \partial_y T_f(x, 0, z) = 0, \quad \partial_y T_f(x, W, z) = 0, \quad \partial_z T_f(x, y, H) = 0. \quad (6)$$

For both geometries, the prescribed pressure drops and absolute temperatures for different simulation cases are summarized in Table 2.

Table 2: Boundary conditions - prescribed values.

HX1				HX2			
	Δp [Pa]	T_{in} [°C]	T_g [°C]		Δp [Pa]	T_{in} [°C]	T_g [°C]
1	5.0	23.00	54.90	1	5.0	23.00	54.90
2	10.0	23.00	43.43	2	10.0	23.00	43.43
3	20.0	23.00	37.20	3	20.0	23.00	37.20
4	40.0	23.00	33.00	4	40.0	23.00	33.00
5	74.7	23.02	30.30	5	74.72	23.02	30.30
6	120.0	23.00	29.00	6	120.0	23.00	29.00
7	175.6	23.02	27.90	7	175.6	23.02	27.90
8	266.5	23.04	27.30	8	200.0	23.04	27.50

5 CALCULATION PROCEDURE

Transport equations (1) and (2) and boundary conditions (4)-(6) were transformed into dimensionless form and discretized according to the finite volume methods ([6] and [7]). Due to boundary conditions, the velocity in the streamwise direction u_f is described as two-dimensional scalar field, whereas the fluid-phase temperature T_f as a three-dimensional scalar field. This resulted in a non-symmetric five diagonal matrix system for two-dimensional scalar field and a seven diagonal matrix system for three-dimensional scalar field.

In order to invert the matrix systems efficiently, a preconditioned conjugate gradient method described in [11] was adopted for this specific problem.

6 RESULTS AND DISCUSSION

The calculations were performed for the pressure drops summarized in Table 2. The pressure drops imposed on the HX1 simulation domain result in fluid flows having the Reynolds numbers from $Re_h = 139$ to 2025, whereas the pressure drops imposed on the HX2 simulation domain result in fluid flows with Reynolds numbers from $Re_h = 546$ to 6691.

Figures 4 and 5 present the cross-sections of the fluid temperature fields for the HX1 and HX2 simulation domains, respectively. These two examples are given for case 7, where

the pressure drop Δp is 175.6 Pa, the inflow temperature T_{in} is 23.02 °C and the bottom temperature is 27.90 °C for both geometries (Table 2).

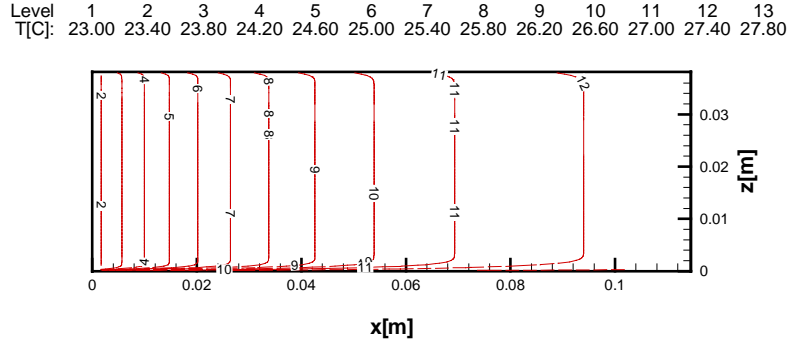


Figure 4: Fluid temperature field in heat exchanger, HX1, Case 7, $Re_h = 1532$.

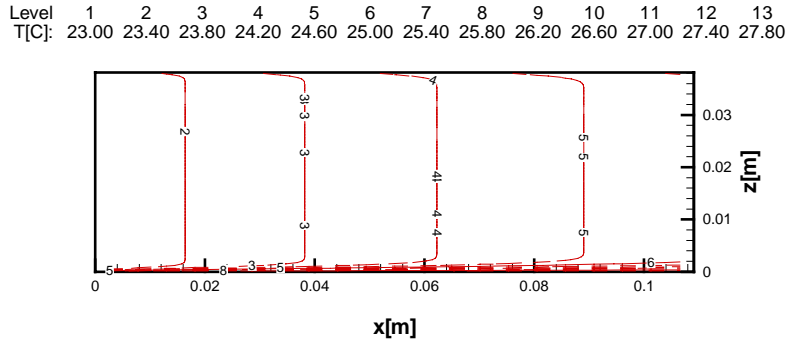


Figure 5: Fluid temperature field in heat exchanger, HX2, Case 7, $Re_h = 5960$.

In Figs. 4 and 5, the temperature field is presented by isolines of constant temperature. The fluid flow is heated by isothermal pin-fins and the bottom wall. Therefore, the fluid temperature gradually increases from the inlet (left side of the figure) to the outlet (right side of the figure). When comparing Figs. 1 and 2, it is evident that the temperature rises much faster in HX1 than in HX2. This is due to denser matrix of pin-fins in HX1 geometry.

Figure 5 also shows intensive heating from isothermal bottom boundary, which results in development of a horizontal thermal boundary layer in passing air. This effect is observed only at HX2 and it is not present at denser matrix of HX1. Based on this observation, we can conclude that in sparse matrices the heat transfer from the bottom is more important than in denser matrices.

The whole-section drag coefficient \bar{C}_d (7) and the whole-section heat permeability $Q/\Delta T$ (8) were calculated and compared with experimental results, where they were available.

$$\bar{C}_d = \frac{2\Delta p}{\rho_f \bar{u}_f^2} \left(\frac{A_c}{A_o} \right) \quad (7)$$

$$\frac{Q}{T_g - T_{in}} = \rho_f c_f \frac{(\bar{T}_{out} - T_{in})}{T_g - T_{in}} A_c \quad (8)$$

Figure 6 shows the comparison between the calculated and experimental values of the whole-section drag coefficient $\overline{C_d}$ for both studied geometries. The calculated values reproduce the experimental data only generally with an error up to 50 per cent. It is believed that discrepancies arise from inadequate boundary conditions for DNS model of REV. Namely, at the REV inflow simple slug flow with uniform velocity u_c was prescribed as a replacement of periodic boundary conditions.

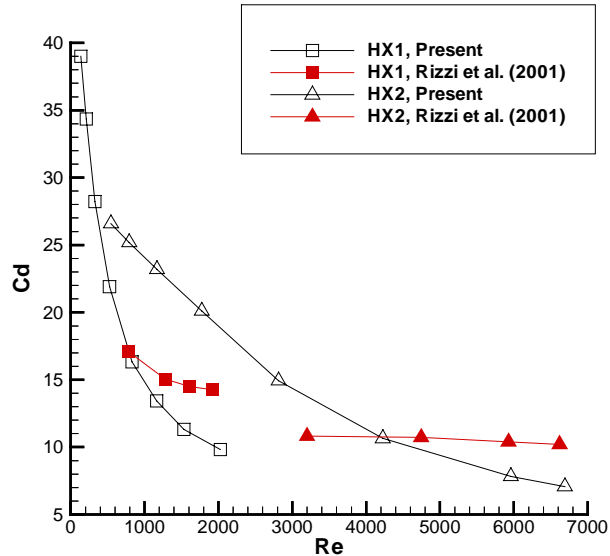


Figure 6: The whole-section drag coefficient C_d .

Figure 7 presents the whole-section heat permeability $Q/\Delta T$ calculated for both geometries HX1 and HX2. As the experimental data of Rizzi et al. [5] were not obtained for isothermal, but for heat conducting structure, they cannot be used for comparison and validation of the overall modeling procedure.

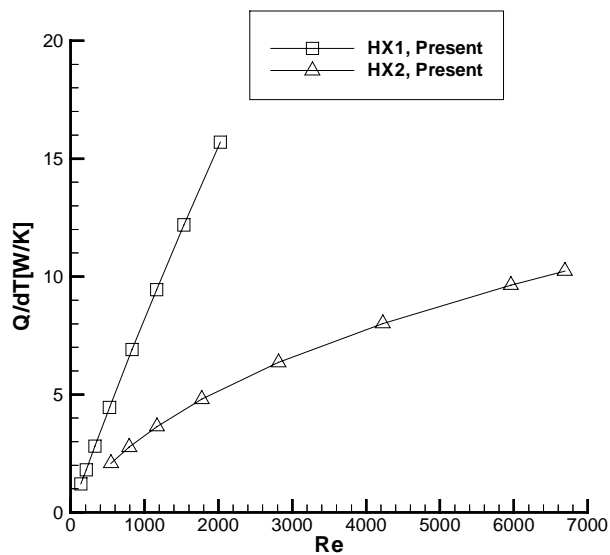


Figure 7: The whole-section heat permeability $Q/\Delta T$.

The diagram in Fig. 7 shows that for the same Reynolds number Re_h the geometry HX1 enables much higher heat flow Q per unit temperature difference ΔT than the geometry HX2. Also, the slopes of both $Q/\Delta T$ curves are different. The $Q/\Delta T$ curve of HX1 shows a linear Reynolds number Re_h dependence, whereas the $Q/\Delta T$ curve of HX2 has a parabolic shape. As such the latter case is much closer to heat transfer in channel flow.

7 SUMMARY

The present paper describes an effort to develop a fast running calculation for simulation of steady-state heat transfer process in a heat exchanger with a generalized geometry. For that purpose the Volume Averaging Technique (VAT) was employed in order to model the heat exchanger cross-flow as a porous media flow. As the averaging of transport equations lead to a "closure" problem, separate relations were introduced to model interphase momentum and heat transfer between fluid flow and the solid structure.

The closure relations contain two additional parameters, the local drag and heat transfer coefficients, which need to be determined. The principles of hierarchic modeling were used to calculate the local drag coefficient C_d as a function of Reynolds number Re_h . For that purpose a separate model of heat exchanger's REV was built and DNS of fluid flow through REV was performed. Due to difficulties to assign the appropriate thermal boundary condition for the REV domain, the local values of heat transfer coefficient were obtained from experimental data of Žukauskas and Ulinskas [2] and Kay and London [3].

The example calculations were made for two different geometries (HX1 and HX2) with staggered pin-fins arrangement cooled with airflow. The geometry of the simulation domain and boundary conditions followed the geometry of the experimental test section used in the Morrin-Martinelli-Gier Memorial Heat Transfer Laboratory at U.C.L.A. . The resulting partial differential equations were discretized using the momentum and energy conservation properties of the finite volume method. The resulting system of semi-linear equations was solved with a preconditioned conjugate gradient method.

The calculated temperature fields revealed that the geometry with denser pin-fins arrangement (HX1) heats fluid flow faster. The temperature field in the HX2 exhibits formation of the thermal boundary layer between pin-fins, which has a significant role in overall thermal performance of the heat exchanger.

The whole-section drag coefficient \bar{C}_d was also calculated and compared with experimental data of Rizzi et al. [5]. The comparison shows up to 50 per cent difference between numerical and experimental results, which is believed to be a consequence of oversimplified momentum equation boundary conditions. Although, the presented discrepancies of the whole-section drag coefficient \bar{C}_d are high, we believe that hierarchic modeling is an appropriate strategy for calculation of complex transport phenomena in heat exchanger geometries.

NOMENCLATURE

A_c	inflow area	T_{out}	outflow temperature
A_o	interface area	u	velocity in streamwise direction
A_w	contact (wetted) area of test section	u_c	inflow velocity
c	specific heat	W	width of simulation domain
C_d	local drag coefficient	x	coordinate in streamwise direction
\bar{C}_d	whole-section drag coefficient	y	coordinate in spanwise direction
d	diameter	z	coordinate in spanwise direction
d_h	hydraulic diameter ($= 4\Omega_f/A_w$)	<i>Subscripts / Superscripts</i>	
h	heat transfer coefficient	f	fluid phase
H	pin-fins height	s	solid phase
H_b	solid base height	x	streamwise direction
L	length of simulation domain	y	spanwise (horizontal) direction
Δp	whole-section pressure drop	z	spanwise (vertical) direction
Δp^*	REV pressure drop	<i>Greek letters</i>	
Q	thermal power	α	phase fraction
Re_h	Reynolds number ($= u_f d_h / \nu_f$)	λ	thermal conductivity
S	specific interface surface ($= A_o / \Omega_f$)	ρ	density
T	temperature	Ω	control volume
T_g	bottom temperature	μ	dynamic viscosity
T_{in}	inflow temperature	ν	kinematic viscosity

REFERENCES

- [1] V., Travkin, I., Catton, "A Two Temperature Model for Fluid Flow and Heat Transfer in a Porous Layer", *J. Fluid Engineering*, Vol. 117, 1995, pp. 181-188.
- [2] A.A., Žukauskas, R., Ulinskas, "Efficiency Parameters for Heat Transfer in Tube Banks", *J. Heat Transfer Engineering*, Vol.5, No.1, 1985, pp. 19-25.
- [3] W.M., Kays, A.L., London, *Compact Heat Exchangers*. 3rd Ed. Krieger Publishing Company, Malabar, Florida, 1998, pp. 146-147.
- [4] A.Horvat, *Calculation of Conjugate Heat Transfer in a Heat Sink Using Volume Averaging Technique (VAT)*, M.Sc. Thesis, University of California, Los Angeles, 2002, www2.ijs.si/~ahorvat.
- [5] M., Rizzi, M., Canino, K., Hu, S., Jones, V., Travkin, I., Catton, "Experimental Investigation of Pin Fin Heat Sink Effectiveness", Proc. of the 35th National Heat Transfer Conference, Anaheim, California, 2001.